

***Ab initio* study of the adsorption, migration, clustering, and reaction of palladium on the surface of silicon carbide**

P. C. Schuck* and R. E. Stoller

Oak Ridge National Laboratory, P.O. Box 2008 MS6138, Oak Ridge, Tennessee 37831, USA

(Received 17 November 2010; revised manuscript received 28 January 2011; published 17 March 2011)

This work presents first principle calculations to understand the adsorption, clustering, migration, and reaction of Pd on three different surfaces of 3C-SiC ($\{111\}$, $\{100\}$ C-terminated, and $\{100\}$ Si-terminated). The surfaces were chosen based upon experimental and theoretical work. Pd preferably binds to Si-terminated surfaces and has higher migration energies on these surfaces. Pd has low migration energies on non-Si-terminated surfaces facilitating the creation of Pd clusters. About 0.5 eV is gained per Pd atom added to a cluster. Reaction mechanisms are reported for Pd reacting on $\{100\}$ surfaces. On the $\{100\}$ C-terminated surfaces, a single Pd atom can substitute for a C with an energy barrier of 0.48 eV and two Pd atoms can substitute for two C atoms with an energy barrier of 0.04 eV. In both cases, the Pd atoms form Pd-C-C bridges between Si lattice sites. For the $\{100\}$ Si-terminated surface, a single Pd atom can substitute for a Si atom with an energy barrier is 1.53 eV. No comparable low energy pathways were found on the $\{111\}$ surface.

DOI: [10.1103/PhysRevB.83.125303](https://doi.org/10.1103/PhysRevB.83.125303)

PACS number(s): 68.35.bg, 31.15.E-, 68.43.-h, 82.40.-g

I. INTRODUCTION

The reaction between palladium and silicon carbide is important for applications in the semiconductor and nuclear industries. In semiconductor applications, Schottky diodes are created by depositing Pd on SiC and are used as hydrogen and hydrocarbon sensors.^{1,2} For nuclear applications, Pd is a fission product from nuclear fuels. Coated particle fuels, such as tristructural-isotropic (TRISO), have a SiC layer that provides structural integrity and Pd will react with SiC to lessen its strength and eventually cause fission product release. Understanding the kinetics and reaction mechanisms of the Pd/SiC system is critical in extending the lifetime of TRISO fuels.

While research has been performed investigating the effects of Pd on TRISO fuel,³⁻⁶ little information is known on the kinetics and reaction mechanisms. Areas of research in Pd/SiC other than TRISO fuels can provide insights on the nature of the reaction. In particular, research for Schottky diodes and the Pd/Si system can provide a framework of information to use as a starting point to perform specific research to determine the kinetics and reaction mechanisms.

Typical research for Schottky diodes involves depositing Pd layers ranging from 0.2 to 100 nm in thickness on SiC free surfaces and annealing at temperatures between 400 °C and 900 °C (Refs. 7-9). At temperatures as low as 500 °C, Pd reacts with SiC to form islands of palladium silicide (predominantly Pd₂Si) surrounded by amorphous graphite. In creating TRISO, SiC is grown on a pyrolytic carbon (PyC) layer in which the interface between SiC and PyC has different chemistry than a free surface of SiC. The question which arises is how applicable is the free surface data of Pd/SiC to TRISO. The answer comes from research performed by Miller *et al.*¹⁰ which showed that the PyC layers contracted when irradiated and debonding occurred between the the PyC and SiC. Thus, SiC is initially in a nonfree surface environment when fabricated, but after irradiation will have free surface characteristics. Therefore, results from free surface work are transferable to TRISO and we expect a similar behavior of Pd clustering into islands of Pd₂Si to occur in TRISO.

Another consideration in comparing the semiconductor and TRISO application is how the Pd is deposited on the surface. Large amounts of Pd are deposited on the surface for semiconductor research. In contrast, during neutron exposure of TRISO, individual atoms are released as a result of fission and diffuse through the fuel kernel, buffer layer, and inner PyC before reaching the SiC. Thus, information is needed on how individual Pd atoms behave on the surface of SiC. Some of this information was gained through research in catalysis that investigated submonolayer Pd deposition on SiC (Refs. 11,12). While results were reported on the characterization of the surface, their primary interest was in the catalytic properties and not the initial surface reaction with Pd. In addition, this research was conducted at room temperature, which is lower than the palladium silicide formation temperature and much lower than TRISO operating temperatures of 1000 °C to 1300 °C. Thus, more information is needed on how small amounts of Pd interact with the surface of SiC.

The Pd/Si system can also provide information for Pd/SiC as the two systems have some similarities. When Pd is deposited on Si and annealed, it also forms islands of Pd₂Si (Ref. 13). The main difference is the temperature at which this occurs; in Pd/Si, Pd₂Si is formed at temperatures as low as 180 K (Ref. 14). The similarities can be understood by investigating the ternary phase diagrams of Pd-Si-C which show no stable Pd-C compounds.^{15,16} The only stable compound with C in the phase diagram is SiC, but the Si prefers to bind with Pd over C as the formation energy of $2\text{Pd} + \text{SiC} \leftrightarrow \text{Pd}_2\text{Si} + \text{C}$ (graphite) is -1.6 eV as determined from our theoretical calculations. This also explains why the Pd/SiC system forms Pd₂Si + graphite as the C can only form compounds with itself since Si prefers Pd. In Pd/Si, the initial reaction between Pd and Si is orders of magnitude faster than the rate-limiting diffusion step.¹⁷ Thus, reactions that occur in the interface between Pd and Si are very fast and not a rate-limiting step. If this extends to Pd/SiC, once the Si is removed from the surface, it will be in a fast reacting interface regime. The diffusion limited step of Pd/Si does not directly apply to TRISO as individual Pd atoms will adsorb on the surface of SiC and migrate along the surface until they reach the fast acting interface regime between SiC

and Pd₂Si. They will not need to diffuse through the Pd₂Si layer to reach the Si. Therefore, we expect the rate-limiting step to be either the removal of Si or C from SiC.

In general, using first principles calculations in combination with experimental research is an effective process to help determine viable reaction mechanisms. Combining the above experimental work shows a macroscopic picture of how the Pd and SiC will react to form Pd₂Si, but underscores the lack of information on the rate-limiting reactions and on how small amounts of Pd atoms behave on the surface. First principle calculations are an excellent tool to gain more information in these areas. To date, only a limited number of papers have used first principle calculations to study interactions between Pd and SiC which primarily focused on bulk SiC (Refs. 18,19). Interpreting the results from those papers leads to the conclusion that the rate-limiting steps of Pd reacting with SiC do not occur in the bulk. Thus, combining the theoretical and experimental results suggests that the rate-limiting reaction occurs on the surface of SiC. Thus, this paper will use first principles calculations to give insights on the adatom adsorption and migration, Pd clustering, and Pd reaction mechanisms on the surfaces in SiC. In addition, we will identify the most important result that the removal of Si from SiC is the rate-limiting step for the reaction of Pd and SiC.

The rest of the paper is outlined as follows. The methodology is presented in Sec. II where we report the computational method, atom configurations for the three surfaces we investigate, and the adsorption energy. In Sec. III we discuss the Pd migration and clustering. Next, the reaction of Pd with the surface of SiC is discussed in Sec. IV. This will be followed by a conclusion.

II. METHODOLOGY

A. Computational method

The first-principles calculations were performed within the framework of density functional theory (DFT) in the local spin-density approximation (LSDA) as implemented by the Vienna *ab initio* simulation package (VASP 4.6)²⁰⁻²². The exchange and correlation energy was treated in the Ceperly and Alder²³ approximation in the parametrization of Perdew and Zunger.²⁴ LSDA was selected because it better represents the formation energies of SiC and Pd₂Si (Ref. 19). The electron-ion interaction is approximated by ultrasoft pseudopotentials developed by Vanderbilt.²⁵ In the case of carbon we used a special soft pseudopotential developed specifically for first row p elements.

To calculate the geometries of 3C-SiC, the atoms were relaxed to their ground state using the conjugate-gradient algorithm such that the errors in the total energy due to lack of self consistency are less than 0.001 eV per unit cell. The plane-wave cutoff was set to 450 eV and a Gaussian smearing of 0.05 eV was used. A $3 \times 3 \times 1$ *k*-point Monkhorst pack²⁶ grid was used to sample the energies. Convergence of 1 meV/atom was reached for both the plane-wave cutoff and *k*-point sampling. Our simulation used periodic boundary conditions and the lattice parameter was 4.3258 Å as found by fitting to the Murnaghan equation of state.²⁷ The migration

energies were calculated by the nudged elastic band method as implemented in VASP.

In the Introduction we reported the formation energy of Pd₂Si for the following reaction, Pd + SiC \rightleftharpoons Pd₂Si + C. Bulk Pd, bulk Pd₂Si, 3C-SiC, and graphite were used for this reaction. We used the same energy cutoff for each of these cells and converged the *k*-point sampling as stated above.

B. Surfaces

The {111} and {100} surfaces are commonly studied both by experiment and theory. We selected surfaces to study that were low energy, consistent with other research, matched both experimental and theoretical conditions when possible, and were reasonable to study through computation.

The commonly accepted most stable surface reconstruction for the {111} is the $(\sqrt{3} \times \sqrt{3})$ (Ref. 29). This surface is Si-terminated with a Si adatom. In TRISO, the SiC is deposited on pyrolytic carbon and not in a Si rich environment. We preferred to use a reconstruction that would more closely resemble the TRISO interface. Research has been done investigating the surface reconstructions on graphene and SiC and they have found a $c(2 \times 2)$ model which we will use.³⁰

The structure of the {100} surface in SiC is composed of alternating layers of Si and C. When Pd attacks the {100} surface, it will have to attack both Si and C layers. Thus, we chose a Si and C-terminated surface for each of these compounds. Unfortunately, some controversy exists in the literature on which surface reconstruction is the lowest energy for each of these surfaces. For {100} C-terminated, the $C(2 \times 2)$ with triple-bonded carbons is the commonly accepted stable structure. For LDA calculations, the $p(1 \times 2)$ is found to have the lowest energy.²⁹ To stay consistent with other LDA calculations and for ease of computations, we selected the $p(1 \times 2)$ termination. For Si terminated SiC, the $p(1 \times 2)$ surface is found to be stable both experimentally and theoretically. Yet, there is disagreement on how the Si atoms are arranged on the surface. Experimentally, the Si are found to form buckled dimers. This is not the case with first principles calculations where only a small contraction is found with the topmost Si. One explanation for the discrepancy is that when the surface is under stress, Si dimers are formed theoretically. Thus, it's possible that through either sample preparation or in an experimental investigation, stress could be added to the surface which would cause Si dimers to form where under more relaxed conditions they would not. For our study, we model an unstressed surface where Si atoms see a small contraction from their perfect lattice sites.

We identified three low energy surfaces from the literature, {100} C-terminated $p(1 \times 2)$, {100} Si-terminated $p(1 \times 2)$ (Ref. 31), and {111} surface $c(2 \times 2)$ (Ref. 30) and show them in Fig. 1. The unit cells are shown by dashed lines. We refer to the {100} surfaces as {100}C and {100}Si for their respective terminations. We used the repeated slab method to create the structures. In all three surfaces, eight layers of SiC were used. The translation vectors of the unit cells were equally increased such that each layer had 16 atoms for a combined total of 128 Si and C atoms in the supercell. The slab on the opposite side

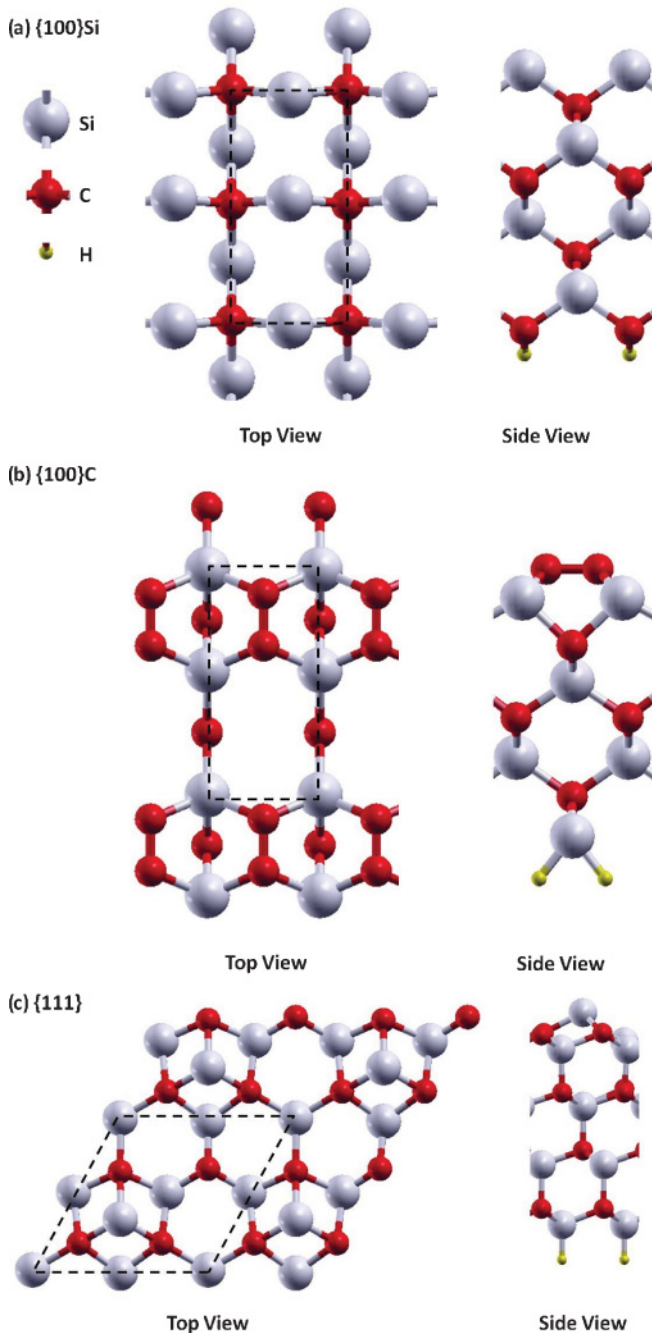


FIG. 1. (Color online) A top and side view for the three surfaces of SiC, (a) $\{100\}$ Si, (b) $\{100\}$ C, and (c) $\{111\}$. For this and subsequent figures, the top view only shows the top three layers of the lattice. The unit cells are highlighted by dashed lines. All atom images were created by the XCRYSDEN software (Ref. 28).

of the surface was terminated with hydrogen atoms to avoid errors from artificial charge transfer. The hydrogen atoms and the four adjacent layers were fixed with bulk parameters and the four layers closest to the surface were allowed to relax. We used a lattice constant of 4.3258 Å. A vacuum was added above the surface and the energy of the structures were converged to 5 meV/Å of vacuum and ranges from 8 to 10 Å for the surfaces.

TABLE I. Adsorption energy (eV) of Pd adatoms on three SiC surfaces ($\{100\}$ C, $\{100\}$ Si, and $\{111\}$). See Fig. 2 for the location of the sites.

Site	$\{100\}$ C	$\{100\}$ Si	$\{111\}$
1	1.55	-1.53	1.04
2	1.46	-1.51	0.93
3	1.54	-1.53	1.04
4	1.46		0.93
5	1.46		1.04
6			0.93

C. Adsorption energy

The adsorption energy is the difference between the energy of the products and the reactants for the chemical reaction of $\text{Pd} + \text{SiC}_{\text{free-surface}} \Leftrightarrow \text{SiC}(\text{Pd})$. The $\text{SiC}_{\text{free-surface}}$ is the calculated energy from the applicable surface in the previous section and $\text{SiC}(\text{Pd})$ is the calculated energy of that same surface with Pd adatoms. The chemical state of Pd is more challenging to characterize. Before reaction with SiC, Pd is embedded in PyC. The energy of this state would be difficult to accurately calculate as the structure of PyC is complex with many possible sites for Pd to occupy. One thing that is certain is that the energy state of Pd is between the energy of bulk Pd (-6.44 eV) and a Pd atom in vacuum (-1.46 eV). We know from experiments in TRISO fuels that Pd attack is favorable and in this work we are more concerned with kinetics and differences in energies such that any errors from the unknown chemical state of Pd would cancel out for these values. With this in mind, we choose bulk Pd as the reference state of Pd.

III. PALLADIUM MIGRATION AND CLUSTERING

Pd adatoms will bind to multiple sites on each of the three surfaces. Table I lists the adsorption energy for a Pd adatom on the surface in several sites. The sites referenced in the table are shown in Fig. 2. In general, Pd does not strongly bind to the $\{100\}$ C and $\{111\}$ compared to the $\{100\}$ Si. These results are expected as we know from the phase diagrams that Pd will bind strongly with Si, but not with C which is more prevalent on the surface in $\{100\}$ C and $\{111\}$. A lower binding energy allows for easier Pd migration on the surface so Pd clusters can form. We discuss the migration energy of Pd adatoms and the energy of Pd clusters in the following sections.

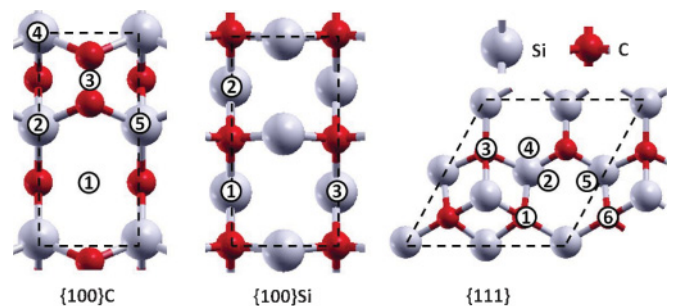


FIG. 2. (Color online) Three surfaces of SiC showing the location of stable sites for Pd adatoms adsorption. The adsorption energy of these adatoms is listed in Table I.

TABLE II. Migration energy barrier (eV) of Pd adatoms on $\{111\}$. The pathway numbers refer to the sites on Fig. 2.

Pathway	Forward	Reverse
1 \rightarrow 2	0.01	0.11
2 \rightarrow 4	0.20	0.20
2 \rightarrow 5	0.45	0.45

A. $\{111\}$

The $\{111\}$ surface has two unique stable sites for Pd. We included four additional sites that are related by symmetry to the first two sites. These latter four sites are needed to calculate the migration of Pd across the surface and to more easily explain its pathway. Table II lists the migration energy between these sites. Pd migrating between the two unique sites 1 and 2 has a maximum energy barrier of 0.11 eV. Pd can migrate from site 2 to 4 with a 0.20 eV barrier. There is no direct path from site 1 to 3, instead the Pd migrates along the pathway 1-2-4-3. For Pd to travel across the surface, it has to migrate to site 5 or 6. Migrating from site 2 to 5 has a 0.45-eV barrier and migration from path 1 to 6 occurs through sites 2-5. Thus, a Pd atom will migrate across the $\{111\}$ surface following the pathway of 3-4-2-5-6 with a maximum barrier of 0.45 eV.

B. $\{100\}C$

We identified three unique stable sites for Pd on $\{100\}C$. Site numbers 4 and 5 are related to site 2 through symmetry. As noted in Table I, all sites have very similar energy and the energy barrier for Pd motion on those sites is at most 0.42 eV. Table III lists the energy barriers for motion between the sites. Pd can traverse across the surface through sites 1-2-4-2-1 or 2-1-5. The largest barrier in either pathway is traveling from site 2 to 1 with an energy barrier of 0.42 eV. Thus, we expect the Pd to easily migrate across the surface.

C. $\{100\}Si$

Two stable sites were identified on $\{100\}Si$. The difference between sites 1 and 2 on the free surface is the separation distance between the Si atoms. The Si atoms adjacent to site 1 are extended and 3.37 Å apart while the Si atoms adjacent to site 2 are contracted and 2.73 Å apart. When Pd is placed on site 1 and relaxed, little change is seen for the geometry of the surface. Yet, when Pd is placed on site 2 and relaxed, the contracted Si atoms are expanded from 2.73 to 3.26 Å. This expansion only occurs to the Si atoms adjacent to Pd and the next set of Pd atoms are closer to their equilibrium value. This change in the surface structure depending on the

TABLE III. Migration energy barrier (eV) of Pd adatoms on $\{100\}C$. The pathway numbers refer to the sites on Fig. 2.

Pathway	Forward	Reverse
1 \rightarrow 2	0.33	0.42
1 \rightarrow 3	0.59	0.60
2 \rightarrow 3	0.21	0.13
2 \rightarrow 4	0.05	0.05
2 \rightarrow 5	0.59	0.59

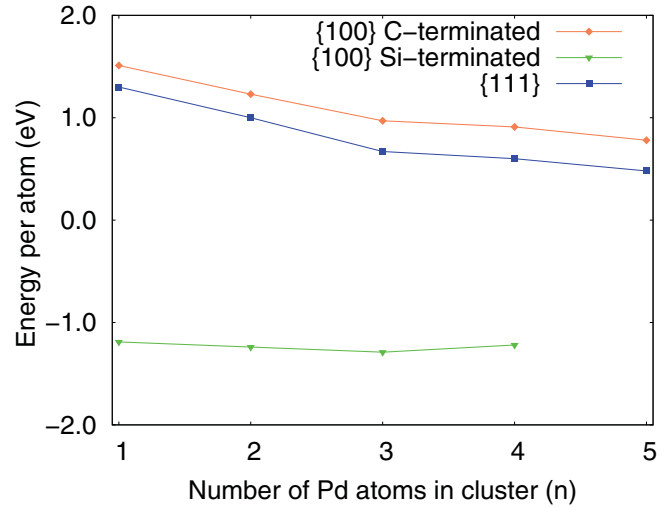


FIG. 3. (Color online) Average energy of Pd in a cluster of size n on three different surfaces of SiC, $\{100\}Si$, $\{100\}C$, and $\{111\}$.

location of the Pd atom has a small effect on the overall energy with a difference of only 0.02 eV. Table IV shows the migration energy for Pd for two possible pathways. The migration energy is highest on this surface with an energy barrier of 0.82 eV. This is due to the stronger binding of Pd on this surface.

D. Palladium clusters

Figure 3 shows the energy results for the Pd clusters on the surfaces. On each of the surfaces, Pd atoms were added individually and relaxed to an energy minimum. The energy difference from a clean surface and one that has Pd atoms was averaged by the number of Pd atoms in the cluster. The results show how the average energy changes as each Pd is added to the cluster. We see two distinct results. For $\{100\}Si$, there is very little change to the overall energy as Pd atoms are added. This occurs because the Pd binds strongly to the Si and does not form tight clusters. For the other two surfaces, Pd binds more strongly to the other atoms in the cluster. As atoms are added to the cluster, they bind more strongly to each other. When the cluster has three atoms or more, 0.5 eV is gained in energy for each atom that is added to the cluster. Figure 4 shows Pd clusters on the three surfaces.

Additional calculations were performed to determine the level of interaction between Pd clusters in adjacent periodic images. A smaller supercell for $\{100\}C$ was created in which each layer was one quarter the size of the original supercell.

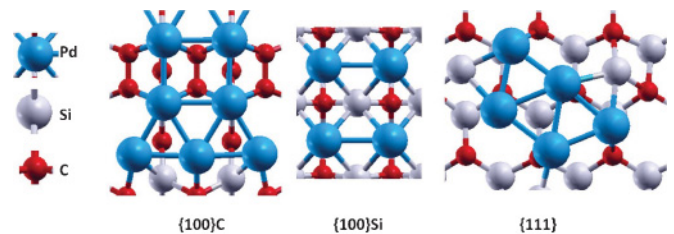


FIG. 4. (Color online) Pd clusters on the $\{100\}C$, $\{100\}Si$, and $\{111\}$.

TABLE IV. Migration energy barrier (eV) of Pd adatoms on $\{100\}$ Si. The pathway numbers refer to the sites on Fig. 2.

Pathway	Forward	Reverse
1 \rightarrow 2	1.39	1.39
1 \rightarrow 3	0.82	0.82

A single Pd atom was placed on the surface and the defect formation energy was calculated and compared to the original sized supercell. Two calculations were performed for Pd on different adsorption sites and the average error was 1%. The distance between Pd atoms in the smaller cell was 6.1 Å which is smaller than the closest distance (6.5 Å) between five atom Pd clusters from the original calculations. Thus, any interaction between periodic images is negligible.

IV. PALLADIUM REACTION

We found multiple pathways for C removal from $\{100\}$ C that required less than 1.5 eV. We report two of the lowest energy pathways that we found; one involves a single Pd atom and the other involves two Pd atoms. The final step in either pathway is similar; the C-C dimer becomes a Pd-C-C bridge. Figure 5 shows the final configuration for a single Pd-C-C bridge. For the single atom, the Pd starts on site 1, and moves toward site 3. The Pd atom will start binding with the Si atoms on site 2 and 5 and push the carbon dimer at site 3 up until it reaches the final configuration as seen in Fig. 5. The energy barrier for this reaction is 0.48 eV with a ΔH (energy difference between products and reactants) of -0.49 eV. This reaction barrier is slightly higher than the rate-limiting step for Pd migration on $\{100\}$ C of 0.42 eV, but much more energy is gained from this reaction and the reverse barrier is 0.97 eV. Thus, as individual Pd atoms migrate across the surface, they have competing mechanisms to migrate or react. Migrating Pd atoms will continue to migrate until they react with the surface. Once they react, they will be in a more stable configuration and less likely to return to migration. Thus, over time the Pd will react with the surface.

With two Pd atoms, the barrier is reduced significantly. The two Pd atoms start in adjacent 1 sites. One Pd atom will repeat the process described for the single Pd atom. The second Pd atom allows for more lattice distortion and reduces the energy

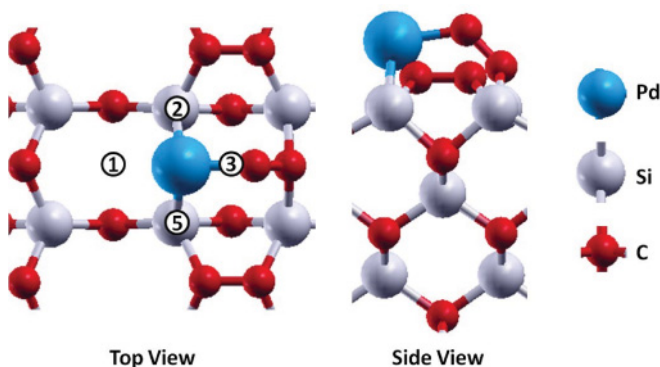


FIG. 5. (Color online) Pd-C-C bridge on $\{100\}$ C surface. The site numbers correspond to the same sites in Fig. 2.

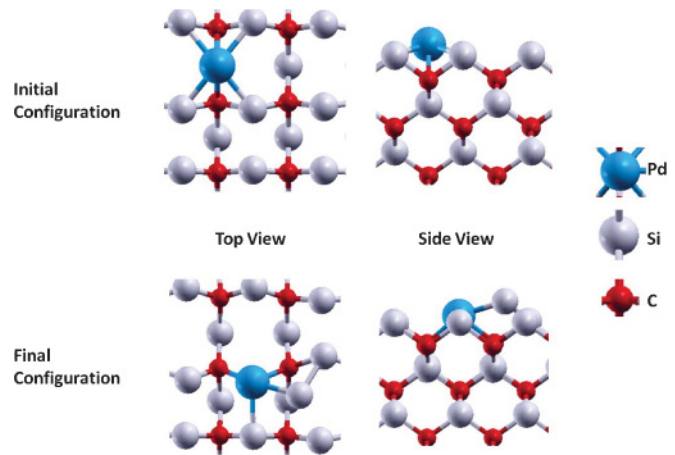


FIG. 6. (Color online) Initial and final configurations for Pd substitution for Si on $\{100\}$ Si.

barrier for this step to 0.04 eV. The second Pd then forms a Pd-C-C bridge adjacent to the first Pd-C-C bridge. There is no energy barrier to the second bridge formation. The total ΔH for these reactions is -1.33 eV. Thus, when Pd atoms migrate and appear in adjacent 1-type lattice sites, a very low energy pathway exists to form double Pd-C-C bridges that are very stable.

To complete the Pd substitution process for C, a C needs to be removed from the Pd-C-C bridge. Unfortunately, we were unable to find a low energy pathway (<5.0 eV) for C removal. As seen from experimental work, the C will eventually reform as amorphous graphite away from the Pd₂Si. The PyC layer is an obvious candidate for the final location of the C atoms as they are displaced from SiC. Experimental work shows amorphous Pd-Si-C structures between the SiC surface and Pd₂Si. This amorphous structure can provide the medium for C migration away from the surface. If the Pd and Si in the Pd-Si-C amorphous layers behave similarly to the Pd/Si system, then this will be a fast reacting regime and will not be a rate-limiting step.

The rate-limiting step is more likely to occur on the $\{100\}$ Si. The Si from this surface is removed by direct substitution. We show the initial and final atomic configurations of this reaction in Fig. 6. The barrier for this reaction is 1.53 eV and the ΔH is 0.76 eV. Pd prefers to be surrounded by Si and in the initial configuration, Pd is bonded to four Si. The final configuration has Pd bonded to two Si and two C. Thus, one would expect the formation energy to be higher for the final state. The energy barrier for the reverse reaction is 0.77 eV which is also close to the migration energy for Pd on this surface. Thus, Pd will have a difficult time reacting with $\{100\}$ Si as single Pd adatoms. While a 1.53 eV barrier sounds reasonable for a reaction that starts to occur at 500 °C, the ΔH needs to be lower for the substitution to be stable. In practice, the SiC surface will be covered with multiple layers of Pd to help stabilize the substitution. We performed calculations with multiple Pd atoms (up to 12 atom clusters) searching for a more stable final state, but were unable to find any. It is possible that a larger cell size with more Pd layers is needed to accurately capture the ΔH .

The {111} surface is stable when in contact with Pd. We were unable to find any low energy pathways (<5.0 eV) in which individual Pd atoms were able to remove C or Si from the surface. We found one pathway in which a cluster of 6 Pd atoms was able to remove a single C atom from the surface with an energy barrier of 3.0 eV and a ΔH of 0.63 eV. This is a high barrier and this reaction would not occur often. One explanation for the difficulty in removing surface atoms from {111} is that the majority of the atoms in {111} have sp^3 bonding and have four bonds to adjacent atoms which is very similar to bulk structure. To remove one of these atoms is comparable to creating a vacancy which has a formation energy of ≈ 4.0 eV (Ref. 18). Thus, the Pd on the {111} surface will be mobile and form Pd clusters, but will not react with the surface. It is uncertain whether this is representative of experiment. There are no papers that investigate Pd deposition on the {111} surface in 3C-SiC. Two papers investigated the {0001} surface in 6H-SiC (Refs. 7,8) which is similar chemically to the {111} in 3C-SiC, yet both of these papers were tested on Si-rich 6H-SiC which is not directly comparable to our surface. With a Si-rich surface a quick reaction is observed between the Pd and Si-rich layers. Upon heating to 600 °C, the Pd starts reacting with the underlying SiC lattice. With energy barriers greater than 3.0 eV for C removal and 5.0 eV for Si removal, the temperature would need to be much greater to see these reactions. Some possible explanations for these results include (1) Pd does not react with the {111} surface, (2) a lower energy barrier exists, but involves a larger interface between Pd and SiC which is beyond our computational ability, and (3) Pd attack occurs on defects on the surface. Explanation 1 is possible and is not disproved by experimental work, yet more experimental work is needed to be able to confirm this. Explanation 2 is very possible and is similar to our explanation for the reaction energies in {100}Si. Explanation 3 is also possible if the attack starts from grain boundaries or grooves in the surfaces and expose a {100} facet within the {111} surface. Thus, the attack would occur from the $\langle 100 \rangle$ instead of the $\langle 111 \rangle$ and have similar energies to the reaction on {100}.

V. CONCLUSION

The Introduction identified two important areas in need of more research to better understand the reaction between Pd and SiC within the context of TRISO fuels. The first area was that little information is known on the reaction with small amounts of Pd on the surface of SiC. The second area was identifying the rate-limiting step of this reaction. First principle calculations were used to address both of these areas. To determine how Pd reacts with the surface of SiC, calculations were performed focusing on the adsorption, clustering, and migration of Pd on three different surfaces of 3C-SiC ({111}, {100}C, {100}Si). The surfaces were chosen based upon experimental and theoretical work. Pd preferably binds to {100}Si with a binding energy of -1.1 eV and migration energy of 0.82 eV. Pd has higher binding energies on {100}C and {111} (≈ 1 eV) and low migration energies of 0.42 eV for {100}C and 0.45 eV for {111}. These low migration energies facilitate the creation of Pd clusters in which ≈ 0.5 eV is gained per Pd atom added to a cluster.

The reaction of Pd with the surface of SiC was also investigated to determine the rate-limiting step. On {100}C, a single Pd atom will substitute for C with an energy barrier of 0.48 eV to form a Pd-C-C bridge. Two Pd atoms will substitute for two C atoms with an energy barrier of 0.04 eV forming adjacent Pd-C-C bridges. For {100}Si, a single Pd atom will substitute for Si with an energy barrier is 1.53 eV and represents a rate-limiting step for conversion of Pd and SiC into Pd₂Si. No comparable low energy pathways were found on the {111} surface.

ACKNOWLEDGMENTS

This work was funded under the US Department of Energy/Nuclear Energy Fuel Cycle Research and Development Deep Burn program with Oak Ridge National Laboratory.

*schuckpc@ornl.gov

¹W. Lu, D. Shi, A. Burger, and W. Collins, *J. Vac. Sci. Technol. A* **17**, 1182 (1999).

²L. Chen, G. Hunter, P. Neudeck, G. Bansal, J. Petit, and D. Knight, *J. Vac. Sci. Technol. A* **15**, 1228 (1997).

³K. Minato, T. Ogawa, S. Kashimura, K. Fukuda, M. Shimizu, Y. Tayama, and I. Takahashi, *J. Nucl. Mater.* **172**, 184 (1990).

⁴T. N. Tieg, *Nucl. Technol.* **57**, 389 (1982).

⁵R. Lauf, T. Lindemer, and R. Pearson, *J. Nucl. Mater.* **120**, 6 (1984).

⁶K. Sawa and S. Ueta, *Nucl. Eng. Des.* **233**, 163 (2004).

⁷I. Tsiaoussis, N. Frangis, C. Manolikas, and T. T. A. N., *J. Cryst Growth* **300**, 368 (2007).

⁸J. Veuillen, T. Tan, I. Tsiaoussis, N. Frangis, M. Brunel, and R. Gunnella, *Diam. Relat. Mater.* **8**, 352 (1999).

⁹C. Pai, C. Hanson, and S. Lau, *J. Appl. Phys.* **57**, 618 (1985).

¹⁰G. Miller, D. Petti, J. Maki, and D. Knudson, *J. Nucl. Mater.* **355**, 150 (2006).

¹¹A. Berthet, A. Thomann, F. Aires, M. Brun, C. Deranlot, J. Bertolini, J. Rozenbaum, P. Brault, and P. Andreazza, *J. Catal.* **190**, 49 (2000).

¹²L. Lianos, A. Berthet, C. Deranlot, E. Aires, J. Massardier, and J. Bertolini, *J. Catal.* **177**, 129 (1998).

¹³M. Takeguchi, K. Mitsuishi, M. Tanaka, and K. Furuya, *Microsc. Microanal.* **10**, 134 (2004).

¹⁴G. W. Rubloff, P. S. Ho, J. F. Freeouf, and J. E. Lewis, *Phys. Rev. B* **23**, 4183 (1981).

¹⁵K. Bhanumurthy and R. Schmid-Fetzer, *Z. Metallkd* **87**, 244 (1996).

¹⁶Z. Du, C. Guo, X. Yang, and T. Liu, *Intermetallics* **14**, 560 (2006).

¹⁷G. Hutchins and A. Shepela, *Thin Solid Films* **18**, 343 (1973).

¹⁸P. Schuck, D. Shrader, and R. Stoller, *Philos. Mag.* **91**, 458 (2011).

¹⁹G. Roma, *J. Appl. Phys.* **106**, 123504 (2009).

- ²⁰G. Kresse and J. Hafner, *Phys. Rev. B* **48**, 13115 (1993).
- ²¹G. Kresse and J. Furthmuller, *Phys. Rev. B* **54**, 11169 (1996).
- ²²G. Kresse and J. Furthmuller, *Comp. Mater. Sci.* **6**, 15 (1996).
- ²³D. M. Ceperley and B. J. Alder, *Phys. Rev. Lett.* **45**, 566 (1980).
- ²⁴J. P. Perdew and A. Zunger, *Phys. Rev. B* **23**, 5048 (1981).
- ²⁵D. Vanderbilt, *Phys. Rev. B* **41**, 7892 (1990).
- ²⁶H. Monkhorst and J. Pack, *Phys. Rev. B* **13**, 5188 (1976).
- ²⁷F. D. Murnaghan, *Proc. Natl. Acad. Sci. USA* **71**, 809 (1944).
- ²⁸A. Kokalj, *Comp. Mater. Sci.* **28**, 155 (2003).
- ²⁹A. Catellani and G. Galli, *Prog. Surf. Sci.* **69**, 101 (2002).
- ³⁰L. Magaud, F. Hiebel, F. Varchon, P. Mallet, and J. Y. Veuillen, *Phys. Rev. B* **79**, 161405 (2009).
- ³¹M. Sabisch, P. Kruger, A. Mazur, M. Rohlfing, and J. Pollmann, *Phys. Rev. B* **53**, 13121 (1996).